December 2001

Direct Imaging of Human SWI/SNF-Remodeled Mono- and Polynucleosomes by Atomic Force Microscopy Employing Carbon Nanotube Tips

Gavin R. Schnitzler
Tufts University School of Medicine, Boston, Massachusetts

Chin Li Cheung
University of Nebraska at Lincoln, ccheung2@unl.edu

Jason H. Hafner
Harvard University, Cambridge, Massachusetts

Andrew J. Saurin
Massachusetts General Hospital, Boston, Massachusetts

Robert E. Kingston
Massachusetts General Hospital, Boston, Massachusetts

See next page for additional authors

MOLECULAR AND CELLULAR BIOLOGY, Dec. 2001, p. 8504–8511 Vol. 21, No. 24
0270-7306/01/$04.00+0 DOI: 10.1128/MCB.21.24.8504–8511.2001

Direct Imaging of Human SWI/SNF-Remodeled Mono- and Polynucleosomes by Atomic Force Microscopy Employing Carbon Nanotube Tips

GAVIN R. SCHNITZLER,[1,2]* CHIN LI CHEUNG,[3] JASON H. HAFNER,[3]† ANDREW J. SAURIN,[2] ROBERT E. KINGSTON,[2] AND CHARLES M. LIEBER[3]*

Department of Biochemistry, Tufts University School of Medicine, Boston, Massachusetts 02111[1]; Department of Molecular Biology, Massachusetts General Hospital, Boston, Massachusetts 02114[2]; and Department of Chemistry and Chemical Biology, Harvard University, Cambridge, Massachusetts 02138[3]

Received 6 July 2001/Returned for modification 8 August 2001/Accepted 19 September 2001

Chromatin-remodeling complexes alter chromatin structure to facilitate, or in some cases repress, gene expression. Recent studies have suggested two potential pathways by which such regulation might occur. In the first, the remodeling complex repositions nucleosomes along DNA to open or occlude regulatory sites. In the second, the remodeling complex creates an altered dimeric form of the nucleosome that has altered accessibility to transcription factors. The extent of translational repositioning, the structure of the remodeled dimer, and the presence of dimers on remodeled polynucleosomes have been difficult to gauge by biochemical assays. To address these questions, ultrahigh-resolution carbon nanotube tip atomic force microscopy was used to examine the products of remodeling reactions carried out by the human SWI/SNF (hSWI/SNF) complex. We found that mononucleosome remodeling by hSWI/SNF resulted in a dimer of mononucleosomes in which ~60 bp of DNA is more weakly bound than in control nucleosomes. Arrays of evenly spaced nucleosomes that were positioned by 5S rRNA gene sequences were disorganized by hSWI/SNF, and this resulted in long stretches of bare DNA, as well as clusters of nucleosomes. The formation of structurally altered nucleosomes on the array is suggested by a significant increase in the fraction of closely abutting nucleosome pairs and by a general destabilization of nucleosomes on the array. These results suggest that both the repositioning and structural alteration of nucleosomes are important aspects of hSWI/SNF action on polynucleosomes.

The wrapping of DNA around histone octamers to form nucleosomes blocks access of DNA binding factors and/or advancing polymerases, resulting in inhibition of transcription, recombination, and replication. In order for these processes to occur, nucleosomes need to be either (i) modified to make them less inhibitory or (ii) moved away from regulatory sequences or advancing polymerases. Two distinct classes of complexes are believed to carry out these functions. Histone acetyltransferases covalently modify histone N termini but do not alter nucleosome positions. In contrast, an evolutionarily conserved family of ATP-dependent nucleosome-remodeling complexes can both noncovalently modify and reposition nucleosomes in chromatin (for reviews, see references 13 and 14).

The SWI/SNF subfamily of remodeling complexes is highly conserved between yeast and humans. Members appear to be functionally conserved in terms of their effects on nucleosomes: where two complexes have been carefully compared, they have almost always shown similar activities (for reviews, see references 13 and 35). Some of the remodeling effects introduced by SWI/SNF complexes are transient, requiring continuous ATP hydrolysis to be observed (18, 19), while others are stable (5, 12, 20, 21, 28, 29, 31, 34). One stable effect is the formation of a novel nucleosome structure that results from SWI/SNF remodeling of mononucleosomes. This structure appears to be a noncovalently bound dimer of nucleosomes, as judged by chromatographic and sedimentation size estimates and the stoichiometry of its components. The DNA in these dimers is thought to wrap around the histone octamers in an altered manner, as judged by changes in DNase, micrococcal nuclease, restriction enzyme, and Gal4 access (20, 31). Very little is known, however, about the altered dimer's gross structure and the mechanism by which it is formed.

SWI/SNF and related complexes also remodel polynucleosomal templates. Several aspects of this remodeling are stable after removal of ATP from the reaction mixture and/or SWI/SNF from the template (for a review, see reference 13). One stable change is seen in a supercoiling assay, in which human SWI/SNF (hSWI/SNF) or yeast SWI/SNF reduces the degree of negative supercoiling of plasmid chromatin without apparent nucleosome loss, suggesting the presence of nucleosomes around which DNA wraps in a nonstandard manner (7, 11, 12, 32). Other stable changes are indicated by alterations in endonuclease cleavage patterns by yeast SWI/SNF (12). Remodeling enhances endonuclease cutting at sites normally blocked by the presence of a nucleosome and diminishes cutting at sites normally free of a nucleosome. Furthermore, on an array of evenly spaced nucleosomes, micrococcal nuclease digestion results in evenly spaced cuts on the DNA, while on yeast SWI/SNF-treated arrays, the cutting appears random. These changes

* Corresponding author. Mailing address for G. R. Schnitzler: Department of Biochemistry, Tufts University School of Medicine, 136 Harrison Ave., Boston, MA 02111. Phone: (617) 636-2441. Fax: (617) 636-2409. E-mail: gavin.schnitzler@tufts.edu. Mailing address for C. M. Lieber: Department of Chemistry and Chemical Biology, Harvard University, 12 Oxford St., Cambridge, MA 02138. Phone: (617) 496-3169. Fax: (617) 496-5442. E-mail: cml@cmliris.harvard.edu.

† Present address: Department of Physics and Astronomy, Rice University, Houston, TX 77005.

suggest that the nucleosome positions in polynucleosomes are altered by remodeling, consistent with the observation that several remodeling complexes have been shown to reposition mononucleosomes (16, 22, 28, 34). However, these assays cannot distinguish between normal and structurally altered nucleosomes and do not provide information about the distribution of nucleosomes throughout individual arrays. One transmission electron microscopic study reported that yeast SWI/SNF could bind arrays at two positions, forming a loop, and that nucleosomes within that constrained loop had altered properties. It is unclear, however, whether these changes would be stable upon the removal of yeast SWI/SNF (2).

Here we have further investigated the structure of hSWI/SNF-remodeled products by using atomic force microscopy (AFM). In AFM, samples are deposited on a flat mica substrate and their structure is imaged by a probe tip that is attached to a force-sensing cantilever. AFM allows direct visualization of individual biological macromolecules, making it ideal for studying the tertiary structure of large, irregular multicomponent biomolecules such as chromatin (1, 17, 30, 36). Standard silicon tips have variable apex diameters, which can change during use, and the resulting variability in resolution can complicate analysis of novel structures. Here we used carbon nanotube AFM tips, which are geometrically well defined, robust, and small in diameter (4, 9), to characterize hSWI/SNF and remodeled products. Our results indicate that hSWI/SNF can form dimers of mononucleosomes with weakened histone-DNA interactions and that it can dramatically alter the positions and stability of nucleosomes on polynucleosomal arrays.

MATERIALS AND METHODS

Nucleosome and hSWI/SNF isolation. Mononucleosomes were isolated from HeLa cells by micrococcal nuclease digestion and glycerol gradient centrifugation (31) (gradient buffer [GGB] contains 20 mM HEPES [pH 7.9], 1 mM EDTA, 180 mM KCl, 0.1% NP-40, and 10 or 30% glycerol), followed by dialysis in TE (10 mM Tris [pH 7.5], 1 mM EDTA). These samples are >90% pure by sodium dodecyl sulfate-polyacrylamide gel electrophoresis and gel shift analysis (data not shown). Concentrations are given as the weight of DNA in the nucleosomes. hSWI/SNF was affinity purified from HeLa cells by virtue of a FLAG tag on its Ini1 subunit (33) and was >50% homogeneous, as estimated by silver staining. For imaging, hSWI/SNF was further purified by glycerol gradient centrifugation as for nucleosomes (see above), except that the gradient buffer contained 50 mM Tris (pH 7.5), 1 mM EDTA, bovine serum albumin (BSA) at 100 μg/ml, and 180 mM KCl with 22 or 30% glycerol.

Assembly of chromatin arrays. A nonradioactive or ^{32}P-end-labeled (Klenow fill-in) nucleosomal array, 5S-G5E4 (27), was formed by salt dialysis with HeLa core histones and dialyzed into TE as described previously (24) with the modifications noted (29). Assembly was verified by electrophoresis on a 1% Tris-acetate-EDTA gel and/or by *Eco*RI digestion of the template, which cuts between 208-bp 5S DNA sequences. Eighty to 90% of the 208-bp *Eco*RI fragments were nucleosomal, corresponding to an average of 9 to 11 nucleosomes per array. However, this is likely to be an underestimate of the nucleosome number since nucleosomes covering *Eco*RI sites prevent cutting and cannot be counted.

Mononucleosome remodeling reactions and separation of products. Remodeling reaction mixtures (200 μl) contained 1 μg (~1.3 nM) of hSWI/SNF fraction and 2 μg (~100 nM) of mononucleosomes in 34 mM KCl–20 mM HEPES (pH 7.9)–0.1 mM phenylmethylsulfonyl fluoride–0.5 mM dithiothreitol–0.1% NP-40–0.05 mM EDTA–2.9 mM $MgCl_2$ and (where indicated) 2 mM ATP/$MgCl_2$. After 2 h at 30°C, the KCl concentration was increased to 233 mM and the reaction products were separated by glycerol gradient centrifugation (10 to 30% GGB). Reactions yielded ~20 to 30% altered dimers and ~70 to 80% mononucleosomes, as measured by gel shift of input reaction mixtures and gradient fractions, followed by ethidium bromide fluorescence staining. For exonuclease III (ExoIII) analysis, dimers and mononucleosomes were labeled by T4 polynucleotide kinase (10 U) and [γ-^{32}P]ATP for 30 min at 37°C in 0.5× GGB with BSA at 100 μg/ml and 7 mM $MgCl_2$. Labeled products were then purified on a 5 to 30% glycerol gradient containing 50 mM Tris (pH 7.5), 1 mM EDTA, and BSA at 100 μg/ml. Bare DNA was prepared from labeled mononucleosomes by phenol extraction and ethanol precipitation. Peak fractions were adjusted to 60 mM KCl–0.1% NP-40–20 mM HEPES (pH 7.9)–5.6 mM $MgCl_2$ and digested with 6 U of ExoIII for 3 or 15 min before stopping with EDTA and purification of the DNA as previously described for DNase digestions (31).

Remodeling of 5S array templates. For analytical restriction assays (see Fig. 3A), 3.4 ng of labeled arrays was incubated at 30°C for 60 min in 25-μl standard hSWI/SNF reaction mixtures (with 4 mM $MgCl_2$, 60 mM KCl, 0.1% NP-40, and other conditions as described previously [31]). We added 200 ng of hSWI/SNF, 0.5 mM ATP/$MgCl_2$, and/or 1 U of apyrase where indicated. We added 20 U of *Sac*I or *Xba*I and stopped samples at 10 and 50 min with sodium dodecyl sulfate stop buffer and proteinase K (31) before separating them by 1.5% agarose–Tris-borate-EDTA electrophoresis. The dried gel was quantitated with a Molecular Dynamics PhosphorImager. For AFM analysis, 200 ng (~2.5 nM) of nonradioactive arrays was remodeled by 250 ng of hSWI/SNF (2.5 nM) as described above but with 3 mM $MgCl_2$ and 2 mM ATP/$MgCl_2$ (where indicated) for 60 or 90 min. The reaction was stopped by addition of EDTA to 5 mM and dialyzed into TE at 4°C. To assay for stable changes (1 week later; see Fig. 3B), 10 μl of each dialyzed reaction mixture was adjusted to 50 mM KCl and 5 mM $MgCl_2$ and digested with 20 U of *Sac*I for 20 min before electrophoresis as described above. Ethidium bromide signals from cut and uncut bands were quantitated on a digital camera adjusted to the linear range.

Preparation of samples for AFM, imaging, and analysis. hSWI/SNF, mononucleosomes, and products were fixed with 0.25% glutaraldehyde at 4°C for 6 h and dialyzed into TE at 4°C overnight with one change of buffer. Remodeled array reaction mixtures were dialyzed into TE and (where indicated) fixed for 1 to 2 h on ice by four- to sixfold dilution into 0.16% glutaraldehyde. A freshly cleaved mica surface was treated for 1 min with 1 mM spermidine or a solution of 0.1% poly-L-lysine, washed with several milliliters of water, and dried under N_2. Samples were deposited for 2 min, rinsed with water, and dried under N_2. The samples were imaged with a Multimode Nanoscope IIIa (Digital Instruments, Santa Barbara, Calif.) in tapping mode in air using carbon nanotube tips (4, 9) and/or silicon tips (for some polynucleosome images where fine-scale resolution of features was not critical) with scan sizes of 0.5 to 2 μm and scan rates of 1 to 2 Hz at a resolution of 512 by 512 pixels. Apparent full widths are overestimates due to the width of the tips, and heights tend to be underestimates due to deformation of the sample (3). Due to these considerations, we report average heights and widths (from measurements of >20 molecules) only as approximate values and compare values only for samples imaged with the same tip. Internucleosomal distances were measured from the positions of the nucleosome centers along the DNA. In all cases, we saw similar results with at least two spreads of each of two independent preparations of nucleosomal samples.

RESULTS

Structure of hSWI/SNF-remodeled mononucleosomes. AFM images of mononucleosomes and hSWI/SNF were recorded to provide well-defined points of comparison for the analysis of remodeled products. HeLa mononucleosomes appeared as roughly spherical structures with an average diameter of ~11 nm (measured as full width at half-maximal height) and an average height of ~4 nm (Fig. 1A). These dimensions are consistent with the crystal structure of similar intact mononucleosomes (23). Approximately half of the nucleosomes had a small tail of proper dimensions to be bare DNA extending <10 nm from the nucleosome. Note that the full widths (at zero height) of nucleosome images are often much greater than 11 nm due to broadening by the finite size of the tip (3). Our recent advances in nanotube tip fabrication have provided individual single-walled nanotube tips (8, 9) that image the mononucleosomes with a full width of only ~16.5 nm, thus demonstrating much higher resolution than the ~23-nm full widths previously reported with standard silicon tips (25). Images of gradient-purified, nearly homogeneous hSWI/SNF reveal that it is a large structure (~25-nm full width at half-maximal height by ~6-nm height) with at least four structural lobes. These measurements are in good agreement with the

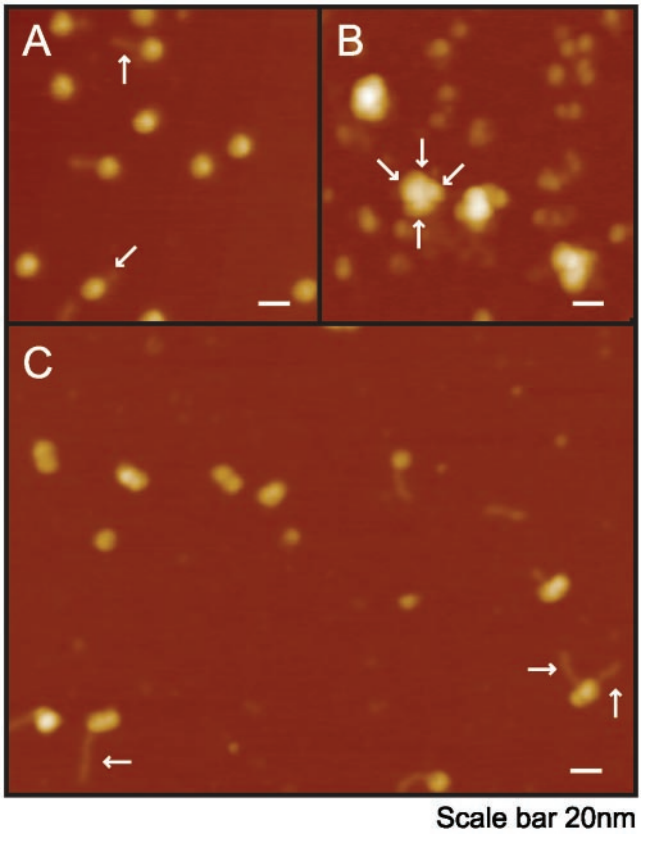

FIG. 1. AFM images of SWI/SNF and altered dimers. Samples were fixed, deposited, and imaged with a nanotube tip as described in Materials and Methods. (A) Mononucleosomes on spermidine-treated mica. DNA tails, where visible, are indicated by arrows. (B) Gradient-purified hSWI/SNF on spermidine-treated mica. Multiple lobes are indicated by arrows. Small molecules are BSA from the gradient buffer. (C) hSWI/SNF-remodeled dimers on poly-L-lysine-treated mica. DNA tails are indicated by arrows.

volume expected for a cylindrical protein with a 2-MDa molecular mass and a 1.3-g/ml density (2,900 nm^3 compared to the 2,600 nm^3 predicted; Fig. 1B), and the width is similar to that seen in transmission electron microscopy pictures of the yeast SWI/SNF complex (2).

In the presence of ATP, hSWI/SNF converts approximately 25% of the input mononucleosomes to altered dimers. Note that not all of nucleosomes are converted to the altered product because hSWI/SNF can also recognize dimers and convert them back to mononucleosomes in an ATP-dependent reaction, thus creating a dynamic equilibrium between mononucleosomes and altered nucleosome dimers. For imaging of SWI/SNF products, nonradioactive mononucleosomes were remodeled by SWI/SNF, and altered dimer products were then separated from mononucleosomes by glycerol gradient centrifugation (31). Reaction mixtures in which the ATP required for SWI/SNF function was omitted were prepared as controls.

Mononucleosome and remodeled dimer nucleosome fractions were isolated from both reaction mixtures with ATP (+ATP) and reaction mixtures without ATP (−ATP), fixed, dialyzed, and deposited on mica for analysis by AFM. The mononucleosome-containing fractions of both the +ATP and −ATP reaction mixtures looked identical to the input mononucleosomes (data not shown), as expected from previous studies (20, 31). Dimer-containing fractions displayed several nucleosome-sized particles that were not present in the −ATP control. The majority of these molecules had two lobes, with each lobe approximating the diameter and height of a single nucleosome (Fig. 1C). The average AFM-measured volume ratio of these molecules to mononucleosomes is 2.2:1, indicating that these structures are dimers of two intact mononucleosomes. Where each lobe was well resolved, the center-to-center distance was 8.9 ± 0.5 nm (standard error of the mean, with a standard deviation of ±2.3 nm; $n = 27$). This spacing nears the theoretical minimum for standard nucleosomes (which are cylinders ~10 nm in diameter and 6 nm in height) and is much closer than that of adjacent nucleosomes on chromatin lacking linker histones (see, e.g., Fig. 4A and references 17 and 36).

Unexpectedly, ~20-nm (60 bp)-long DNA tails were observed on 85% of the altered nucleosome dimers (Fig. 1C and data not shown). By contrast, we observed no tails (50%) or very short (~5- to 10-nm, 15- to 30-bp) tails on the input and −ATP control nucleosomes (Fig. 1A). Short tails would be predicted for the mononucleosomes used here, since almost all of their DNA (146 out of ~155 ± 5 bp) would be bound by histones in the standard conformation (23). Thus, the ~60-bp tails frequently observed in the altered nucleosome dimers indicate a significant unwrapping of DNA from the surface of the fixed histone octamers. The fixation conditions used result in the complete cross-linking of histones to each other but not to the DNA (data not shown), and this might allow weakly bound DNA to be pulled from the histone octamer onto the charged mica surface. Thus, these tails could either represent free bare DNA extending from dimers in solution or a region of weak histone-DNA contacts.

Exo,III is a good probe for bare DNA ends since it digests from the 3′ end of DNA until its progress is blocked by bound protein. The mononucleosome and dimer fractions imaged as described above were end labeled with polynucleotide kinase and separated from free label by gradient centrifugation. These were then subjected to ExoIII digestion for 3 or 15 min (Fig. 2). ExoIII readily cleaves bare DNA to small sizes (lanes 1 to 3). Very little free DNA is available to ExoIII on mononucleosomes, so ExoIII cleavage products are only ~10 to 20 bp shorter than undigested samples (lanes 4 to 6). The DNA on the remodeled dimers appears to be even more resistant to ExoIII digestion than that on mononucleosomes, indicating that remodeling does not generate DNA ends that are free in solution (lanes 7 to 9). This is consistent with previous findings on the digestion of dimers with DNase and micrococcal nuclease (31). Thus, the ~60-bp DNA tails observed on dimers by AFM most likely represent regions of DNA that are more weakly bound to the histone surface than in normal nucleosomes and which are more readily removed to the charged mica surface upon deposition.

5S Arrays are stably remodeled by hSWI/SNF. At its most basic level, cellular chromatin consists of arrays of nucleosomes on the DNA fiber. By comparison to mononucleosomes, little is known about the stable products of SWI/SNF on polynucleosomal arrays. To study this, we used salt dialysis to assemble nucleosomes onto the 5S-G5E4 DNA template, which contains five 5S-rRNA gene (rDNA) sequences (which

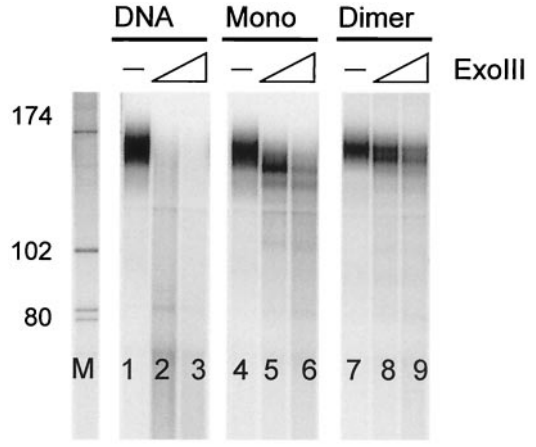

FIG. 2. ExoIII digestion of hSWI/SNF products. 5′-end-labeled remodeled dimers (lanes 7 to 9) and control mononucleosomes (lanes 4 to 6) or bare DNA from mononucleosomes (lanes 1 to 3) were digested with ExoIII for 3 (lanes 2, 5, and 8) or 15 (lanes 3, 6, and 9) min before DNA purification and resolution by denaturing polyacrylamide gel electrophoresis. The values on the left are molecular sizes in base pairs.

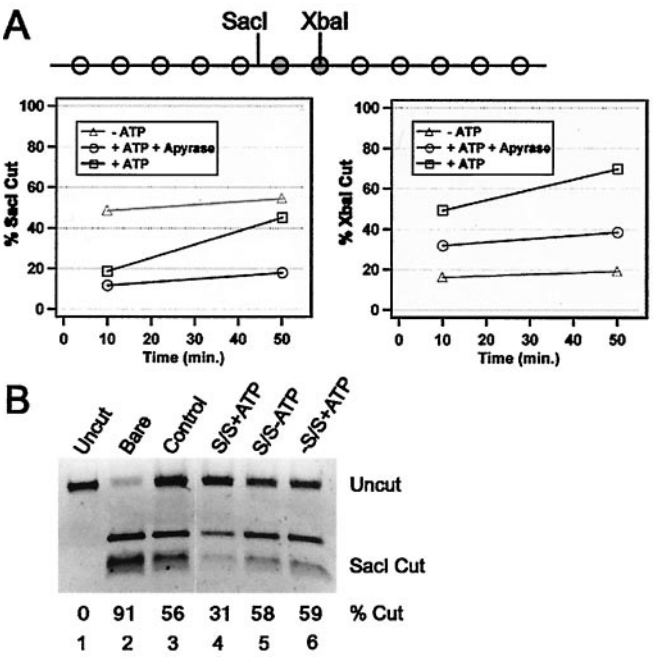

FIG. 3. 5S nucleosomal arrays are stably remodeled by hSWI/SNF. (A) Diagram of the 5S-G5E4 rDNA array used. White circles represent nucleosomes at preferred sites on 208-bp 5S rDNA sequences. Grey circles represent nucleosomes in the transcription template. Locations of *Sac*I and *Xba*I sites relative to inferred unremodeled nucleosome positions are indicated. For the graphs, the array was treated with hSWI/SNF without ATP (triangles), with ATP for 30 min (squares), or with ATP for 30 min, followed by apyrase for 18 min (circles), and then cut with *Sac*I (left) or *Xba*I (right) for the indicated times. The purified DNA was separated by agarose electrophoresis, and percent cutting was quantified. Similar results were obtained in three separate experiments. (B) Unlabeled arrays were incubated with both SWI/SNF (S/S) and ATP (lane 4), without ATP (lane 5), or without SWI/SNF (lane 6) for 90 min before dialysis into TE. Samples of these reaction mixtures and bare DNA (lane 2) or the untreated assembled array (lane 3) were digested with *Sac*I, purified, and separated as described above, followed by ethidium bromide staining and quantitation. Lane 1 contained uncut DNA.

each tend to position a single nucleosome in a preferred location) flanking each side of a transcriptional reporter DNA sequence that accommodates two nucleosomes (diagram in Fig. 3A) (27). The transcriptional reporter sequence contains a unique *Sac*I site that is generally not covered by a nucleosome. Under control conditions, this can be seen as rapid digestion (in the first 10 min) of ~50% of the templates, in which nucleosome positions have left the *Sac*I site bare, followed by much slower digestion of the templates in which the *Sac*I site is covered by a nucleosome (Fig. 3A, left panel, triangles). By contrast, the *Xba*I site is generally nucleosomal, resulting in less than 20% cleavage of the templates in the first 10 min (Fig. 3A, right panel, triangles).

We used *Sac*I and *Xba*I digestion to establish that hSWI/SNF could introduce changes in these polynucleosomes that were stable in the absence of continued SWI/SNF function. 5S-G5E4 nucleosomal arrays were first remodeled by SWI/SNF in the presence of ATP for 30 min. Remodeling was then stopped by the addition of apyrase, which rapidly hydrolyzes the ATP required for SWI/SNF function, and reaction mixtures were incubated for another 18 min. Restriction enzyme was then added, and incubation was continued for 10 or 50 min. The results of this experiment (Fig. 3, compare control triangles to circles) indicate that nucleosome positions have been stably altered by SWI/SNF to more frequently cover the *Sac*I site (decreasing the initial cutting percentage without changing the subsequent rate of cutting) and leave the *Xba*I site bare (increasing the initial cutting percentage). The maintenance of this change does not require further SWI/SNF action, since ATP has been removed by apyrase. The stability of these changes was further confirmed by analyzing unlabeled samples prepared for AFM analysis by dialysis into TE and after several days at 4°C (Fig. 3B). The decrease in *Sac*I cutting on remodeled arrays (lane 4) over controls (lanes 3, 5, and 6) shows that the apparent change in nucleosome positions is stable under the conditions used for imaging. While similar observations have been made for yeast SWI/SNF on other array templates (12), this is the first demonstration of stable changes in nucleosome positions by hSWI/SNF.

In addition to these stable changes in the arrays, we also detected an increase in the rate of digestion of nucleosomes when SWI/SNF, ATP, and the restriction enzyme were present together. We observed two effects when SWI/SNF and ATP were incubated with the template for 30 min, followed immediately by addition of the restriction enzyme (Fig. 3A, squares). First, the percentage of templates cut in the first 10 min changes in accordance with the stable effects described above (increased cutting at *Xba*I and decreased cutting at *Sac*I). Second, the rate of cutting after the first 10 min is increased, indicating that the complex is continually altering nucleosomes to make them more accessible than in the controls.

AFM of SWI/SNF-remodeled 5S arrays. AFM images of fixed, control polynucleosomal arrays (lacking either ATP or SWI/SNF) clearly show the nucleosomes evenly spaced over the DNA (Fig. 4A and data not shown). Analysis of the positions of all of the nucleosomes on 20 arrays yielded an average of 12.5 ± 0.3 nucleosomes per array with an average center-

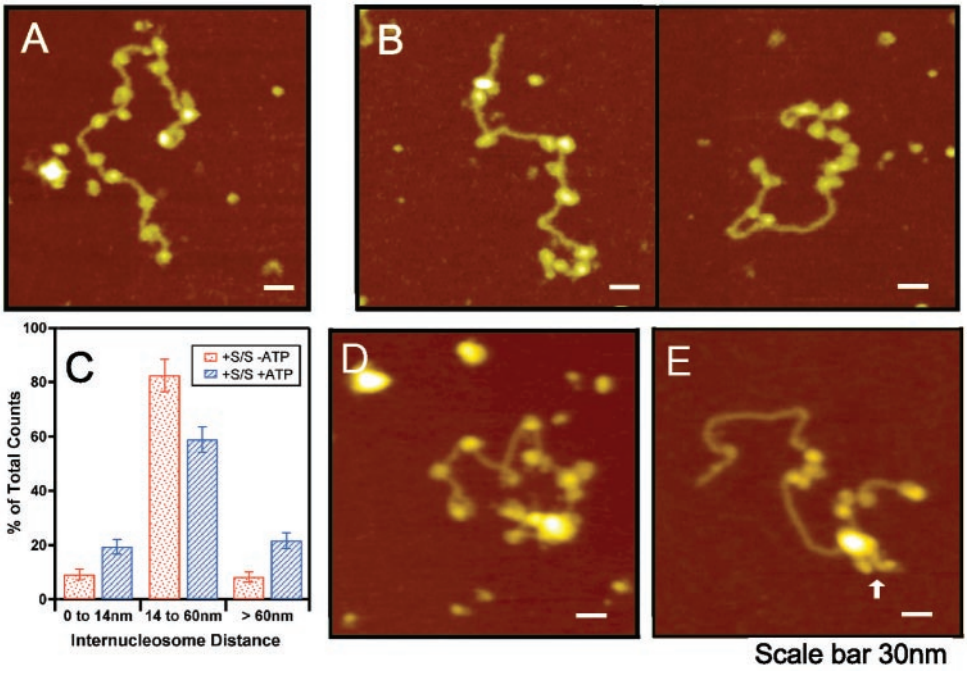

FIG. 4. AFM images of fixed, hSWI/SNF (S/S)-remodeled arrays on spermidine-treated mica. (A) An array from the control reaction mixture lacking ATP (Fig. 3B, lane 5). (B) Arrays remodeled by hSWI/SNF and ATP for 90 min (Fig. 3B, lane 4). (C) Histogram of internucleosomal distances (peak to peak along the DNA contour) from two experiments. The data (23 arrays with ATP, 19 arrays without ATP) were grouped into three bins (≤14 nm, 14 to 60 nm, and >60 nm) and normalized to 100%. (D) An hSWI/SNF-bound array from the same control reaction mixture as in panel A. (E) An hSWI/SNF-bound remodeled array from the same reaction mixture as in panel B. The arrow shows potential DNA loops constrained by SWI/SNF. The height range in panels D and E is greater than in that in panels A and B to allow structural features of SWI/SNF to be evident.

to-center distance of 33 ± 2 nm. The theoretical distance between two nucleosomes at the preferred DNA position on the 208-bp 5S rDNA nucleosome-positioning sequence, assuming 146 bp bound by a 10-nm nucleosome particle and 62 bp (~21 nm) of linker DNA, is 31 nm, in good agreement with our analysis. High-definition mapping studies have shown that nucleosomes occupy their preferred position on 5S rDNA sequences only ~60% of the time (6, 26), which would result in only ~36% of internucleosomal distances matching the theoretical value. This is consistent with the high standard deviation (±22 nm, as distinct from the standard error of the mean noted above) for center-to-center distances observed in our direct imaging experiments.

Incubation with SWI/SNF and ATP resulted in a visually dramatic alteration of polynucleosome structure (Fig. 4B), with an increase in nucleosome clusters and long stretches of bare DNA. Under these reaction conditions, few arrays were bound by SWI/SNF, allowing us to easily examine stable changes in the array that do not require SWI/SNF binding. The remodeling effect of SWI/SNF on the nucleosome positions is quantified and summarized in Fig. 4C. The percentage of nucleosome separations of greater than 60 nm is increased over twofold (from 8% ± 2% to 22% ± 3%), demonstrating that SWI/SNF can move nucleosomes to create long stretches of bare DNA. The percentage of nucleosome separations of 14 nm or less is also more than doubled (from 9% ± 2% to 19% ± 3%), demonstrating that SWI/SNF creates pairs of closely abutting nucleosomes. The average nucleosome count for remodeled arrays was 12.0 ± 0.4, which did not differ significantly from that of controls, and the overall contour length did not change significantly (459 ± 12 nm versus 455 ± 14 nm for the controls). Thus, changes in spacing are not due to nucleosome loss or changes in array length.

To determine whether SWI/SNF remodels arrays progressively or all at once, we compared arrays remodeled for 10 min to those remodeled for 90 min. By the *Sac*I assay, the population of arrays treated with SWI/SNF for 10 min was remodeled to 70% of the level of arrays treated for 90 min. From AFM images of these arrays and controls (+SWI/SNF, −ATP), the number of nucleosome pairs on each individual array that were ≤14, >60, or >80 nm apart was determined. For ease of comparison, we set the average number of pairs per array in each class after 90 min at 100% remodeled and the number in the −ATP control at 0% remodeled. Intriguingly, the number of nucleosome pairs per array spaced >60 nm apart is maximal after 10 min (111% ± 17%), while the more extreme separations (>80 nm apart) are at only 48% ± 21% of maximal levels, and closely abutting pairs (<=14 nm apart) are at only 35 ± 26% of the maximal levels after 10 min. If each SWI/SNF molecule remodeled each array all at once, with the rate of remodeling determined by the rate of initial SWI/SNF binding, then all changes in spacing for the population of arrays should occur at the same rate. By contrast, these results suggest that individual arrays reach a mature remodeled state by progressive action of the complex over time. Whether this is the continued work of a single processive complex or due to multiple hit-and-run remodeling events is unknown.

By focusing on arrays that were not bound by SWI/SNF, as

described above, we could examine the stably remodeled state of the chromatin. We also examined the arrays (20 to 30% of the total) that were bound by structures with the proper dimensions and shape to be SWI/SNF. Representative images of hSWI/SNF-bound arrays from reaction mixtures without and with ATP are shown (Fig. 4D and E, respectively). Roughly half of the time, under both conditions, the bound SWI/SNF complex appears at the base of short protrusions that could potentially be small loops of bare or nucleosome-bound DNA (arrow). This is consistent with an earlier electron micrographic study of yeast SWI/SNF bound to polynucleosomes (2), although we rarely observed clear multinucleosome hSWI/SNF-constrained loops. hSWI/SNF might also be capable of linking multiple arrays, perhaps by binding two DNA sequences at once, since 22% (3 out of 13) of the SWI/SNF-bound polynucleosomal structures from the +ATP reaction mixture were overlapping arrays, compared to only 4% (1 out of 24) of the non-SWI/SNF-bound structures in the same samples. While these counts are too low to be statistically significant, we did note that the SWI/SNF complex was always one of the contact sites in overlapping SWI/SNF-bound arrays. We saw no linked arrays in the −ATP controls (out of 22), which may be due to random chance.

Images of unfixed remodeled arrays reveal instability of remodeled nucleosomes. When arrays of nucleosomes are deposited on charged surfaces and imaged without fixation, they had properties similar to those of fixed arrays, with only a slight reduction in the nucleosome count (e.g., see reference 36). Consistent with those studies, we found that unfixed control arrays treated with SWI/SNF but not ATP looked similar to the fixed arrays (compare Fig. 5A to Fig. 4A) but had a significantly reduced nucleosome count of 10.7 ± 0.5 (n = 10). The spacing of nucleosome pairs on unfixed control arrays was similar to that on fixed control arrays (4% ± 2% ≤14 nm, 76% ± 9% 14 to 60 nm), except that the loss of nucleosomes from the unfixed arrays resulted in an increased frequency of greatly separated pairs (20% ± 4% >60 nm), with a corresponding increase in overall length (517 ± 14 nm). Surprisingly, unfixed remodeled arrays looked strikingly different from both fixed remodeled arrays and unfixed controls (compare Fig. 5B with Fig. 4B and 5A). Clear nucleosome particles were rare, and the DNA was frequently looped or kinked, making it nearly impossible to follow its path. Such a tangle might be expected if the DNA had been pulled from the histones onto the surface. This result indicates that, in addition to altered positions, the stability of the nucleosomes in hSWI/SNF-remodeled arrays is dramatically reduced.

DISCUSSION

In this study, AFM imaging with high-resolution carbon nanotube probes revealed the product formed by SWI/SNF from mononucleosomes to be two closely joined particles equal in size to the input nucleosomes (Fig. 1), which is consistent with a previous biochemical analysis (31). The observation of long DNA tails on dimers (Fig. 1C), combined with the results of exonuclease III digestion (Fig. 2), suggests that 60 to 70 bp of DNA is more weakly associated with histones in dimers than in normal nucleosomes. This fraction of weakened histone-DNA contacts may explain why remodeled dimers are less resistant to disruption by salt than are normal nucleosomes (20; G.R.S., unpublished data). It has been argued that SWI/SNF-like complexes may release 60 to 80 bp of DNA from the surface of the nucleosome (22). Our results suggest, instead, that this length of DNA is associated with histones in an alternative, weaker conformation.

The hSWI/SNF complex (Fig. 1B) is seen as a multilobed structure with apparent twofold symmetry and often with a distinct saddle shape. Transmission electron microscopy pictures of the yeast SWI/SNF complex bound to polynucleosomes, while revealing less about the surface structure of the complex, did show two DNA-nucleosome binding sites per molecule, suggestive of a similar symmetry (2). The details visible in the images presented here suggest that carbon nanotube AFM might be an excellent method for studying the placement and function of subunits and conformational changes in the complex during substrate binding and catalysis.

SWI/SNF dramatically alters the positions of nucleosomes in polynucleosomes compared to those of control arrays (Fig. 4). The frequency of internucleosomal distances of greater than 60 nm are more than doubled, as is that of distances of less than 14 nm. At the same time, the frequency of internucleosomal distances around the 30-nm range, established by the strong 5S rDNA positioning sequences, decreases significantly. These observations provide an explanation for the stable changes in restriction enzyme access introduced by hSWI/SNF or yeast SWI/SNF into arrays of nucleosomes (12) (Fig. 3). These data do not tell us whether SWI/SNF only moves nucleosomes until further movement is blocked by adjacent nucleosomes or whether it can allow histone octamers to be transferred in *cis* past other nucleosomes or even in *trans* to other DNAs, as suggested by other studies (21, 29, 34). We did not observe a significantly broader distribution of the number of nucleosomes per DNA molecule, however, which might be expected if a large number of nucleosomes were removed from some DNAs and deposited on others in *trans*.

Despite alterations in nucleosome positions, the overall length of the arrays does not change, suggesting that the length of DNA associated with each remodeled nucleosome remains the same. This argues against the hypothesis that 60 to 80 bp of DNA is unwound from the ends of remodeled nucleosomes in arrays (22), since this would be predicted to increase array length by over 200 nm. Transmission electron microscopy studies of polynucleosomes remodeled by yeast SWI/SNF indicated an average loss of ~40 bp of DNA from each nucleosome within loops of chromatin physically constrained by SWI/SNF but not from those outside these loops (2). In this study, nucleosomes in arrays not bound by SWI/SNF also appear to have a normal DNA content. We cannot address the nature of nucleosomes in hSWI/SNF-constrained loops, since the potential DNA loops we observed (Fig. 4D and E) were too small.

The increase in closely abutting nucleosomes (14 or fewer nm apart) after hSWI/SNF action could result from either (i) nucleosomes simply being moved close together or (ii) the creation of pairs of altered nucleosomes similar to altered mononucleosome dimers. The analysis of remodeled dimers (Fig. 1C) showed that the center-to-center distance between the two nucleosome lobes was 14 nm or less (2 standard deviations above the average). This analysis, however, did not allow positive identification of similar products on arrays, since each

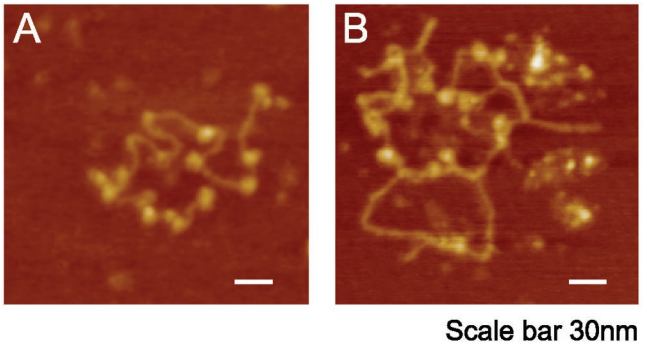

FIG. 5. AFM images of unfixed remodeled arrays suggest reduced nucleosome stability. (A) Control arrays (shown fixed in Fig. 4A) were deposited on spermidine-treated mica without fixation. (B) Remodeled arrays (shown fixed in Fig. 4B) were deposited on spermidine-treated mica without fixation. The small molecules in the background are BSA.

lobe was indistinguishable from normal mononucleosomes in shape and dimensions. Note that, since each measurement on the array represents a pair of nucleosomes, a 10% increase in internucleosome distances of 14 nm or less corresponds to an ~20% increase in nucleosomes with a neighboring nucleosome (on either side) close enough to be part of an altered pair. This fits well with the distribution of SWI/SNF products formed from mononucleosomes, which is generally ~75% mononucleosomes and ~25% dimers at apparent equilibrium. Theoretically, dimers need not be formed between adjacent nucleosomes but might also form between a distant nucleosome pair in *cis* (creating loops) or nucleosomes on two arrays (creating linked arrays). We did not observe a significant increase in these types of structures with remodeled arrays, suggesting that, if dimers are formed, such events might be relatively rare or unstable.

The fact that unfixed remodeled arrays are much less stable than control arrays under our deposition conditions indicates that the nucleosomes on the array have been qualitatively altered and not just repositioned (Fig. 5). Dimers formed from mononucleosomes have been shown to have reduced resistance to dissociation by high salt concentrations (20; G.R.S., unpublished data) and appear to have weaker histone interactions with ~60 bp of associated DNA (Fig. 1C). Thus, an accumulation of dimers on the array might explain the reduced stability of remodeled arrays. It has also been proposed that ATP-dependent chromatin remodeling might involve the formation of distorted single nucleosomes that constrain loops or bubbles of DNA unbound by histones (10). Such changes might also reduce the resistance of the nucleosomes to deposition conditions. They might also lead naturally to the formation of dimers or higher-order multimers that might stabilize distorted nucleosomes against reversion to the normal structure.

hSWI/SNF is involved in transcriptional activation through steroid receptors, heat shock factor, and globin gene regulators, as well as transcriptional repression through the retinoblastoma protein Rb (for reviews, see references 13 and 35). Our observations, summarized in the model proposed in Fig. 6, indicate that hSWI/SNF can accomplish a dramatic restructuring of arrays of nucleosomes to generate both long stretches of

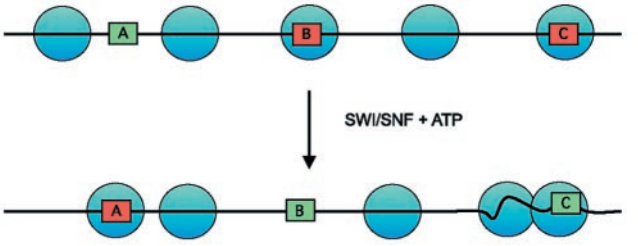

FIG. 6. Model for SWI/SNF remodeling of arrays. Nucleosomes in initial positions (top) block some transcription factor binding sites (B and C) while leaving others open. SWI/SNF alters nucleosome positions (bottom) to uncover some sites (B) and cover others (A). In this way, SWI/SNF remodeling can facilitate both activation and repression. Nucleosome dimers are also formed, which are more accessible to some factors (site C).

bare DNA and clumps of nucleosomes even on DNA harboring strong nucleosome positioning sequences. Thus, the complex may have great power to disrupt and reshuffle nucleosome organization over promoters and transcribed regions in vivo. If the original organization was repressive, this could result in transcriptional activation, either by moving nucleosomes away (e.g., Fig. 6, site B) or by creating distorted mononucleosomes or altered dimers (e.g., Fig. 6, site C), which can be more accessible than normal nucleosomes to transcription and recombination factors (15, 31). If the original organization was active, however, SWI/SNF could result in repression, as nucleosomes are moved over or near transcription factor binding sites (e.g., Fig. 6, site A). Note that in the continued presence of SWI/SNF, nucleosome positions and conformations would be fluid. These changes might be fixed either by the removal of SWI/SNF or by the binding of factors that act as boundaries to nucleosome movement or stabilize one form of the nucleosome (altered or normal) over the other.

Clearly, many questions remain unanswered. How do our present observations relate to the effects of hSWI/SNF on chromatin in vivo, which, for instance, exists with linker histones in a more highly compacted form? Do the changes introduced by hSWI/SNF (dimer formation, repositioning, or both) revert back to normal, and at what rate? How might the complex be regulated, for instance, to promote an active conformation at one promoter and a repressive conformation at another? Members of the ISWI-based family of remodeling complexes aid the regular spacing of nucleosomes. Do these complexes work to counteract complexes like hSWI/SNF that appear adept at disorganization? In seeking answers to all of these questions, and others, we see great potential in a combination of biochemical and molecular imaging techniques.

ACKNOWLEDGMENTS

We thank J. Workman for providing plasmid p2085S-G5E4. We also thank Natasha Ulyanova and members of the Kingston laboratory for comments on this work and the manuscript.

This work was funded by NIH grants to G.R.S., R.E.K., and C.M.L. and an AFOSR grant (F49620-00-1-0084) to C.M.L.. J.H.H. is the recipient of an NIH postdoctoral fellowship (F32 NS10706). A.J.S. is a fellow of the Human Frontier Science Program.

REFERENCES

1. **Allen, M. J.** 1997. Atomic force microscopy: a new way to look at chromatin. IEEE Eng. Med. Biol. Mag. **16:**34–41.

2. **Bazett-Jones, D. P., J. Cote, C. C. Landel, C. L. Peterson, and J. L. Workman.** 1999. The SWI/SNF complex creates loop domains in DNA and polynucleosome arrays and can disrupt DNA-histone contacts within these domains. Mol. Cell. Biol. **19:**1470–1478.
3. **Bustamante, C., and C. Rivetti.** 1996. Visualizing protein-nucleic acid interactions on a large scale with the scanning force microscope. Annu. Rev. Biophys. Biomol. Struct. **25:**395–429.
4. **Cheung, C. L., J. H. Hafner, and C. M. Lieber.** 2000. Carbon nanotube atomic force microscopy tips: direct growth by chemical vapor deposition and application to high-resolution imaging. Proc. Natl. Acad. Sci. USA **97:**3809–3813.
5. **Cote, J., C. L. Peterson, and J. L. Workman.** 1998. Perturbation of nucleosome core structure by the SWI/SNF complex persists after its detachment, enhancing subsequent transcription factor binding. Proc. Natl. Acad. Sci. USA **95:**4947–4952.
6. **Dong, F., J. C. Hansen, and K. E. van Holde.** 1990. DNA and protein determinants of nucleosome positioning on sea urchin 5S rRNA gene sequences in vitro. Proc. Natl. Acad. Sci. USA **87:**5724–5728.
7. **Guyon, J. R., G. J. Narlikar, E. K. Sullivan, and R. E. Kingston.** 2001. Stability of a human SWI-SNF remodeled nucleosomal array. Mol. Cell. Biol. **21:**1132–1144.
8. **Hafner, J., C. L. Cheung, T. H. Oosterkamp, and C. M. Lieber.** 2001. High-yield fabrication of individual single-walled nanotube probe tips for atomic force microscopy. J. Phys. Chem. B **105:**743–746.
9. **Hafner, J. H., C.-L. Cheung, and C. M. Lieber.** 1999. Direct growth of single-walled carbon nanotube scanning probe microscopy tips. J. Am. Chem. Soc. **121:**9750–9751.
10. **Havas, K., A. Flaus, M. Phelan, R. Kingston, P. A. Wade, D. M. Lilley, and T. Owen-Hughes.** 2000. Generation of superhelical torsion by ATP-dependent chromatin remodeling activities. Cell **103:**1133–1142.
11. **Imbalzano, A. N., G. R. Schnitzler, and R. E. Kingston.** 1996. Nucleosome disruption by human SWI/SNF is maintained in the absence of continued ATP hydrolysis. J. Biol. Chem. **271:**20726–20733.
12. **Jaskelioff, M., I. M. Gavin, C. L. Peterson, and C. Logie.** 2000. SWI-SNF-mediated nucleosome remodeling: role of histone octamer mobility in the persistence of the remodeled state. Mol. Cell. Biol. **20:**3058–3068.
13. **Kingston, R. E., and G. J. Narlikar.** 1999. ATP-dependent remodeling and acetylation as regulators of chromatin fluidity. Genes Dev. **13:**2339–2352.
14. **Krebs, J. E., and C. L. Peterson.** 2000. Understanding "active" chromatin: a historical perspective of chromatin remodeling. Crit. Rev. Eukaryot. Gene Expression **10:**1–12.
15. **Kwon, J., K. B. Morshead, J. R. Guyon, R. E. Kingston, and M. A. Oettinger.** 2000. Histone acetylation and hSWI/SNF remodeling act in concert to stimulate V(D)J cleavage of nucleosomal DNA. Mol. Cell **6:**1037–1048.
16. **Langst, G., E. J. Bonte, D. F. Corona, and P. B. Becker.** 1999. Nucleosome movement by CHRAC and ISWI without disruption or trans-displacement of the histone octamer. Cell **97:**843–852.
17. **Leuba, S., C. Bustamante, K. van Holde, and J. Zlatanova.** 1998. Linker histone tails and N-tails of histone H3 are redundant: scanning force microscopy studies of reconstituted fibers. Biophys. J. **74:**2830–2839.
18. **Logie, C., and C. L. Peterson.** 1997. Catalytic activity of the yeast SWI/SNF complex on reconstituted nucleosome arrays. EMBO J. **16:**6772–6782.
19. **Logie, C., C. Tse, J. C. Hansen, and C. L. Peterson.** 1999. The core histone N-terminal domains are required for multiple rounds of catalytic chromatin remodeling by the SWI/SNF and RSC complexes. Biochemistry **38:**2514–2522.
20. **Lorch, Y., B. R. Cairns, M. Zhang, and R. D. Kornberg.** 1998. Activated RSC-nucleosome complex and persistently altered form of the nucleosome. Cell **94:**29–34.
21. **Lorch, Y., M. Zhang, and R. D. Kornberg.** 1999. Histone octamer transfer by a chromatin-remodeling complex. Cell **96:**389–392.
22. **Lorch, Y., M. Zhang, and R. D. Kornberg.** 2001. RSC unravels the nucleosome. Mol. Cell **7:**89–95.
23. **Luger, K., A. W. Mader, R. K. Richmond, D. F. Sargent, and T. J. Richmond.** 1997. Crystal structure of the nucleosome core particle at 2.8 A resolution. Nature **389:**251–260.
24. **Luger, K., T. J. Rechsteiner, A. J. Flaus, M. M. Waye, and T. J. Richmond.** 1997. Characterization of nucleosome core particles containing histone proteins made in bacteria. J. Mol. Biol. **272:**301–311.
25. **Martin, L. D., J. P. Vesenka, E. Henderson, and D. L. Dobbs.** 1995. Visualization of nucleosomal substructure in native chromatin by atomic force microscopy. Biochemistry **34:**4610–4616.
26. **Meersseman, G., S. Pennings, and E. M. Bradbury.** 1991. Chromatosome positioning on assembled long chromatin. Linker histones affect nucleosome placement on 5 S rDNA. J. Mol. Biol. **220:**89–100.
27. **Neely, K. E., A. H. Hassan, A. E. Wallberg, D. J. Steger, B. R. Cairns, A. P. Wright, and J. L. Workman.** 1999. Activation domain-mediated targeting of the SWI/SNF complex to promoters stimulates transcription from nucleosome arrays. Mol. Cell **4:**649–655.
28. **Owen-Hughes, T., R. T. Utley, J. Cote, C. L. Peterson, and J. L. Workman.** 1996. Persistent site-specific remodeling of a nucleosome array by transient action of the SWI/SNF complex. Science **273:**513–516.
29. **Phelan, M. L., G. R. Schnitzler, and R. E. Kingston.** 2000. Octamer transfer and creation of stably remodeled nucleosomes by human SWI-SNF and its isolated ATPases. Mol. Cell. Biol. **20:**6380–6389.
30. **Sato, M. H., K. Ura, K. I. Hohmura, F. Tokumasu, S. H. Yoshimura, F. Hanaoka, and K. Takeyasu.** 1999. Atomic force microscopy sees nucleosome positioning and histone H1-induced compaction in reconstituted chromatin. FEBS Lett. **452:**267–271.
31. **Schnitzler, G., S. Sif, and R. E. Kingston.** 1998. Human SWI/SNF interconverts a nucleosome between its base state and a stable remodeled state. Cell **94:**17–27.
32. **Schnitzler, G. R., S. Sif, and R. E. Kingston.** 1998. A model for chromatin remodeling by the SWI/SNF family. Cold Spring Harbor Symp. Quant. Biol. **63:**535–543.
33. **Sif, S., P. T. Stukenberg, M. W. Kirschner, and R. E. Kingston.** 1998. Mitotic inactivation of a human SWI/SNF chromatin remodeling complex. Genes Dev. **12:**2842–2851.
34. **Whitehouse, I., A. Flaus, B. R. Cairns, M. F. White, J. L. Workman, and T. Owen-Hughes.** 1999. Nucleosome mobilization catalysed by the yeast SWI/SNF complex. Nature **400:**784–787.
35. **Workman, J. L., and R. E. Kingston.** 1998. Alteration of nucleosome structure as a mechanism of transcriptional regulation. Annu. Rev. Biochem. **67:**545–580.
36. **Yodh, J. G., Y. L. Lyubchenko, L. S. Shlyakhtenko, N. Woodbury, and D. Lohr.** 1999. Evidence for nonrandom behavior in 208-12 subsaturated nucleosomal array populations analyzed by AFM. Biochemistry **38:**15756–15763.